AFRL-RX-WP-TP-2009-4082

MULTI-SCALE CHARACTERIZATION OF INHOMOGENEOUS MORPHOLOGICALLY TEXTURED MICROSTRUCTURES (PREPRINT)

J.E. Spowart, G.B. Wilks, and M.A. Tschopp

Metals Branch
Metals, Ceramics and NDE Division

APRIL 2009

Approved for public release; distribution unlimited.

See additional restrictions described on inside pages

STINFO COPY

AIR FORCE RESEARCH LABORATORY
MATERIALS AND MANUFACTURING DIRECTORATE
WRIGHT-PATTERSON AIR FORCE BASE, OH 45433-7750
AIR FORCE MATERIEL COMMAND
UNITED STATES AIR FORCE

REPORT DOCUMENTATION PAGE

Form Approved
OMB No. 0704-0188

1. REPORT DATE *(DD-MM-YY)*
April 2009

2. REPORT TYPE
Journal Article Preprint

3. DATES COVERED *(From - To)*
01 April 2009 – 01 April 2009

4. TITLE AND SUBTITLE
MULTI-SCALE CHARACTERIZATION OF INHOMOGENEOUS MORPHOLOGICALLY TEXTURED MICROSTRUCTURES (PREPRINT)

5a. CONTRACT NUMBER
In-house

5b. GRANT NUMBER

5c. PROGRAM ELEMENT NUMBER
62102F

6. AUTHOR(S)
J.E. Spowart (AFRL/RXLMD)
G.B. Wilks (AFRL/RXLM / General Dynamics)
M.A. Tschopp (AFRL/RXLM / Universal Technology Corporation)

5d. PROJECT NUMBER
4347

5e. TASK NUMBER
RG

5f. WORK UNIT NUMBER
M02R4000

7. PERFORMING ORGANIZATION NAME(S) AND ADDRESS(ES)

Metals Branch (RXLMD)
Metals, Ceramics and NDE Division
Materials and Manufacturing Directorate
Wright-Patterson Air Force Base, OH 45433-7750
Air Force Materiel Command, United States Air Force

General Dynamics, Inc.
Dayton, OH 45431

Universal Technology Corporation
Dayton, OH 45432

8. PERFORMING ORGANIZATION REPORT NUMBER
AFRL-RX-WP-TP-2009-4082

9. SPONSORING/MONITORING AGENCY NAME(S) AND ADDRESS(ES)
Air Force Research Laboratory
Materials and Manufacturing Directorate
Wright-Patterson Air Force Base, OH 45433-7750
Air Force Materiel Command
United States Air Force

10. SPONSORING/MONITORING AGENCY ACRONYM(S)
AFRL/RXLMD

11. SPONSORING/MONITORING AGENCY REPORT NUMBER(S)
AFRL-RX-WP-TP-2009-4082

12. DISTRIBUTION/AVAILABILITY STATEMENT
Approved for public release; distribution unlimited.

13. SUPPLEMENTARY NOTES
To be submitted to Materials Science & Engineering A
PAO Case Number and clearance date: 88ABW-2009-1169, 25 March 2009.
The U.S. Government is joint author on this work and has the right to use, modify, reproduce, release, perform, display, or disclose the work.

14. ABSTRACT
A computationally efficient microstructure characterization technique is presented that separately identifies morphological texture and any orientation dependence of second-phase clustering via a concise visual representation. This technique, the Vector Multi-Scale Analysis of Area Fractions (VMSAAF), is then applied to computer-generated microstructures to understand the effects of second-phase area fraction, aspect ratio, alignment propensity, variant orientation, and degree of microstructure banding on the homogenous length scale – a metric used to quantify clustering – as well as the extent of representative volume elements for a microstructure.

15. SUBJECT TERMS
multi-scale, characterization, clustering, morphology, representative volume element

16. SECURITY CLASSIFICATION OF: a. REPORT	b. ABSTRACT	c. THIS PAGE	17. LIMITATION OF ABSTRACT:	18. NUMBER OF PAGES
Unclassified	Unclassified	Unclassified	SAR	14

19a. NAME OF RESPONSIBLE PERSON (Monitor)
Jonathan Spowart

19b. TELEPHONE NUMBER *(Include Area Code)*
N/A

Standard Form 298 (Rev. 8-98)
Prescribed by ANSI Std. Z39-18

Multi-Scale Characterization of Inhomogeneous Morphologically Textured Microstructures

G. B. Wilks,[a,b,*] M. A. Tschopp,[a,c] J. E. Spowart[a]

[a]*Air Force Research Laboratory, Materials and Manufacturing Directorate (AFRL/RXLM), Wright-Patterson Air Force Base, OH 45433, USA*

[b]*General Dynamics Inc., Dayton, OH 45431, USA*

[c]*Universal Technology Corporation, Dayton, OH 45432, USA*

A computationally efficient microstructure characterization technique is presented that separately identifies morphological texture and any orientation dependence of second-phase clustering via a concise visual representation. This technique, the Vector Multi-Scale Analysis of Area Fractions (VMSAAF), is then applied to computer-generated microstructures to understand the effects of second-phase area fraction, aspect ratio, alignment propensity, variant orientation, and degree of microstructure banding on the homogenous length scale—a metric used to quantify clustering—as well as the extent of representative volume elements for a microstructure.

Keywords: Multi-Scale; Characterization; Clustering; Morphology; Representative Volume Element

1.) Introduction

The effect of second-phase inhomogeneity (clustering) on transport properties and mechanical behavior in heterogeneous material systems has necessitated the development of metrics for quantifying this characteristic so that generalizations can be made about its effect on properties. One way of characterizing homogeneity is through statistically representative length scales or volume elements (RVEs) describing the extent of a microstructure [1-5]; such techniques based on area or volume fraction of the second phase are not only useful for determining the minimum size of accurate microstructure representations (models), but also show strong sensitivity to clustering and, in fact, are excellent metrics for characterizing inhomogeneity since uniform microstructures are unambiguously described by smaller representative elements than those that are clustered [1].

Numerous researchers have illustrated the influence of variations in second-phase homogeneity and associated representative length-scales on material properties, particularly with regard to mechanical behavior in discontinuous composite systems. For example, Borbély *et al* [6] measured short-length scale volume fraction fluctuations in a 20 %-Al_2O_3 (by volume) aluminum-matrix composite via microtomography in order to derive a microstructure correlation length and, consequently, a geometric RVE. Accompanying simulations revealed that the RVE necessary to obtain accurate effective plastic behavior was on the order of twice the size of the RVE necessary to capture the correct elastic response. Likewise, through finite element analysis of actual microstructures obtained from a 30.0%- SiC aluminum matrix composite, Spowart [7] showed that clustering of reinforcement had a significant effect on the yield strength and strain-hardening of the material even though the effect on elastic behavior was relatively minor. Faber and Evans analyzed and experimentally verified that second-phase clustering in a ceramic matrix composite—as defined by a deviation from a uniform distribution for a given volume fraction—resulted in a significant increase in toughness due to crack deflection and twist [8,9]. Using deformation processing to breakdown reinforcement clusters in a 27.5 %-SiC aluminum matrix composite, Wilks manipulated the extent and anisotropy of the RVE for the material, and observed that a smaller RVE correlated with (i) an increase in nearest-neighbor separation, (ii) a larger length scale for the ductile fracture process, and (iii) a substantial increase in the fracture toughness regardless of orientation [10].

Absent from many studies on properties and metrics for characterizing homogeneity though is the ability to quantify clustering and its effects in the presence of morphological texture (alignment) of the second phase. In such material configurations, preferential directions of clustering that can cause significant anisotropy in transport percolation or localization of mechanical response are expected and worth identifying in addition to simpler scalar quantities that measure inhomogeneity like a representative length scale or RVE. Understanding and quantifying clustering in anisotropic materials is therefore the subject of this particular work.

*Corresponding author. Tel.: +1-937-255-5007; fax: +1-937-255-3007; e-mail: garth.wilks@wpafb.af.mil.

2.) Background

Consider the multi-scale analysis of area fractions (MSAAF) technique [1], which identifies a representative length scale for a two-phase microstructure by measuring the variance (σ) of second-phase area fraction between different microstructure sub-regions as a function of length-scale/size of the sub-region (Q). As an example, the *isotropic* form of the MSAAF technique is applied to a synthetic microstructure in Fig. 1, where an array of square sub-regions (of edge-length Q) is used to subdivide the material domain. Expressed as a coefficient of variation (ψ), this variance of second-phase area fraction over all microstructure sub-regions has been shown to obey the relationship [11]

$$\psi = \sigma \big/ A_f = 1 \Big/ \sqrt{A_f \big/ \left(1 - A_f\right) + \alpha\left(Q-1\right)^{-2\xi}} \quad (1)$$

where A_f is the second-phase area fraction, ξ is a "cluster parameter" sensitive to the distribution of the second phase *and* the shape of the measuring sub-region (~ -1.0 for square sub-regions), and α is a "texture parameter" which is mainly sensitive to second-phase morphology and alignment. Since ψ decreases as Q increases, any two-phase microstructure can be characterized by that length scale at which a specified minimum variation in A_f is attained. This *homogeneous length scale*[1] ($Q = L_H$) is a practical metric for quantifying homogeneity in isotropic materials since clustered microstructures are described by larger values of L_H than a homogeneous microstructure of equal second-phase area fraction. This is illustrated in Eq. 1, by the fact that—when all other microstructure features are held constant—clustering is manifested by an increase in ξ, and a corresponding increase in L_H [1].

Quantifying homogeneity in *anisotropic* materials is more complicated, but can be assessed by a *directional* MSAAF technique [11] that decomposes a microstructure image into lineal (strip) elements of length Q (Fig. 1). Since the variation of A_f in such an ensemble of sub-regions also obeys Eq. 1 (with $\xi \sim$ -0.5), this technique can be used to determine *directional* homogeneous length scales[2], L_{Hi}. Three orthogonal values of $L_{H\text{-}i}$ (i = 1,2,3) can be used to define a representative volume element (RVE) for a microstructure the volume of which is described by

$$V_{RVE} = L_{H-1} L_{H-2} L_{H-3} \quad (2)$$

The extent and anisotropy of such an RVE has been shown to be strongly sensitive to second-phase

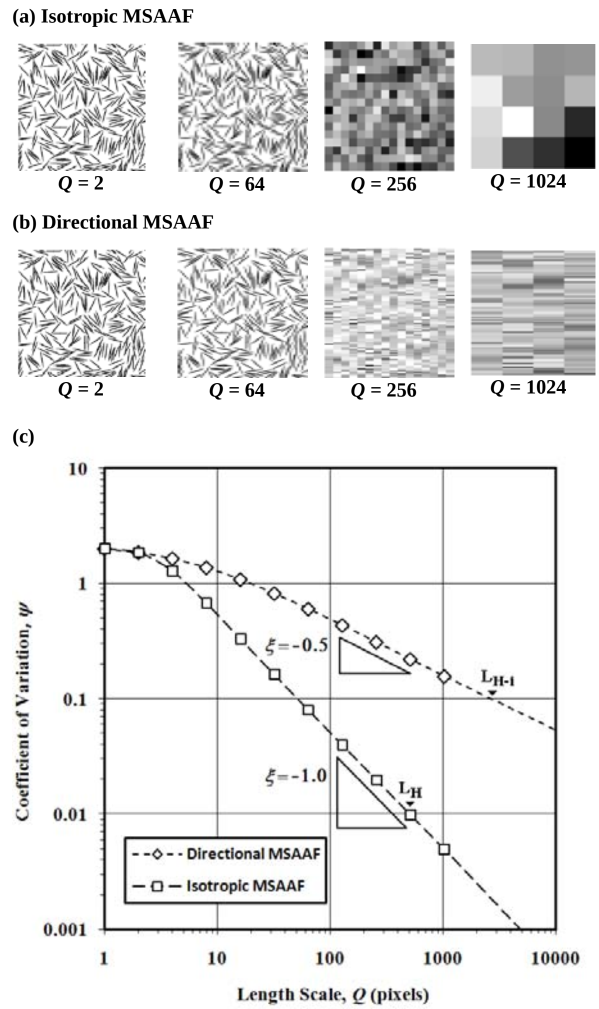

Fig. 1. Illustrations of the (a) isotropic and (b) directional MSAAF technique and (c) the resulting multi-scale behaviour of variation in area fraction for a synthetic microstructure containing A_f = 20% of randomly oriented 16:1 aspect ratio particles—gray level is scaled to indicate local second-phase area fraction.

characteristics (aspect ratio, alignment propensity, etc.) which are manifested primarily through variation in the "texture parameter" α for each $L_{H\text{-}i}$ [11].

3.) Technique

The principal drawback of RVEs constructed using three orthogonal representative length scales is that such an element, by itself, cannot deconvolve the separate effects of second-phase alignment and clustering, or the directional dependence of either quantity. Moreover, if such an element is not aligned with principal directions in a microstructure (e.g. an axis of alignment), variations in the extent of the RVE could be misleading regarding the level of clustering in the material under study. Therefore, in this work, we introduce a *Vector* MSAAF (VMSAAF) technique in which microstructure images are

[1] While the magnitude of the uncertainty depends on the application, in this work, L_H refers to the length scale (Q) at which ψ = 0.01

[2] Caution should be used when comparing values of L_H and L_{Hi} due to the strong dependence of ξ on the dimensionality of the measuring sub-region. For this reason, directional length scales like L_{Hi} refer to the value of Q at which ψ = 0.1

incrementally rotated prior to the application of the directional MSAAF technique so that the multi-scale behavior of second-phase area fractions as a function of the angle of rotation/microstructure direction (θ) can be determined. Results of this technique are presented (e.g., fig. 2) as polar-contour plots of $\psi(\theta)$ where the radial direction is identical to $\mathrm{Log}_{10}(Q)$. Color is scaled such that L_H is denoted by black. Least-square fits to $\psi(\theta)$ are used to determine the texture and cluster parameters (α and ξ, respectively) as functions of θ, and these fits are plotted in conjunction with VMSAAF results. A software tool for applying this analysis to microstructure images has recently been made available [12].

The efficacy of the VMSAAF technique is demonstrated in this work by its application to synthetic two-dimensional microstructures generated by random sequential adsorption (RSA) without simulated annealing [11]. Particle characteristics were varied to produce microstructures with permutations of chosen factor levels, including: second-phase area fraction (A_f = 10%, 20%, 30%), aspect ratio (AR = 4, 8, 16), and the alignment propensity of particle major-axes—*randomly oriented*, *fully aligned*, or *semi-aligned*. The *semi-aligned* conditions being where the orientation of all particle major axes is normally distributed about the direction of alignment ($\theta = 0^o$) with a standard deviation of 20^o. Synthetic microstructure generation began by specifying particle dimensions[3] (in pixels) for each aspect ratio and calculating the number of particles necessary to obtain the prescribed area fraction. To minimize any effect of particle size (area), this factor was kept constant through all conditions. Particle orientation was then randomly sampled from the predetermined orientation distribution while coordinates of particle centroids were subsequently selected via random number generator. Periodic boundaries were used to mitigate edge effects while geometric criteria rejected overlapping particles. Resulting microstructures contained at least 4000 particles and were 4096x4096 pixels in extent[4].

Additional conditions were created to explore the multi-scale behavior of microstructures containing two distinct orientation variants with a fixed misorientation (30^o, 45^o, 60^o, and 90^o) between the particle major axes of each variant. These conditions contained A_f = 20% of a 8:1 aspect ratio second-phase, and were generated in a manner similar to that previously described except the sampled orientation distribution contained only the two variants with each variant equally weighted.

[3]Though absolute length scale is arbitrary in these synthetic microstructures, since features dimensioned in pixels may seem unphysical, the reader may wish to consider a scale of 1 pixel = 1μm.

[4] Although sub-regions (sized ~L_H) are used to illustrate subsequent results, analyses were performed on original (full-size) images.

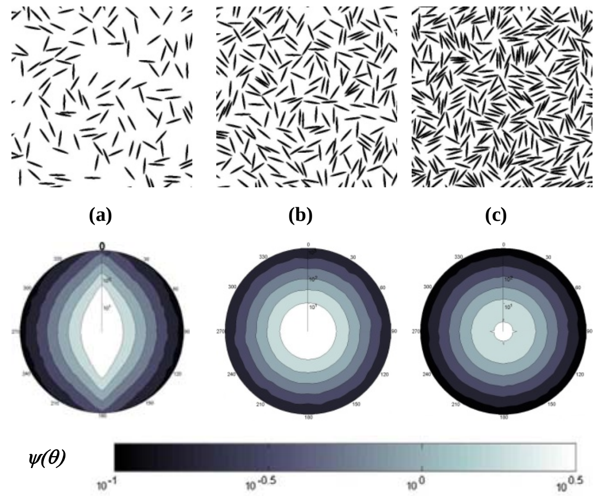

Fig. 2. Randomly oriented microstructures **(top)** containing A_f = **(a)** 10 % **(b)** 20 %, and **(c)** 30 % second-phase with an aspect ratio of 8:1 as well as the corresponding VMSAAF/$\psi(\theta)$ plots **(bottom)**.

Banded microstructures were also created to assess the interaction of second-phase clustering and alignment. The character of the clustering was somewhat arbitrary, being based on the microstructure easiest to generate. Such microstructures were generated by applying a meso-scale mask to remove particles and thereby create rarefied bands in a previously generated (aligned) microstructure containing A_f = 30% of 8:1 aspect ratio particles. Particles were removed from the dense and rarefied regions at different rates until a global area fraction of 20 % was obtained; the width of dense (d) to rarefied (r) regions was controlled to be d/r = 0.0, 0.5, 2.0, and contained area fractions in the dense/rare regions of 20%/20%, 28.5%/15.0%, and 27.4%/3.8%, respectively.

4.) Results & Discussion

The effects of basic microstructure factors on VMSAAF results are congruent with results from other multi-scale analyses. For example, in Fig. 2 the VMSAAF technique concisely illustrates the general inverse relationship that exists between the homogeneous length scale, L_H ,and A_f for randomly aligned microstructures—as A_f increases, L_H decreases [1]. The compound effect of variation in aspect ratio and alignment propensity on the anisotropy of L_H is captured in Fig. 3, which confirms the observation that an increase in particle aspect ratio in an aligned microstructure simultaneously increases L_H in the direction of alignment and decreases L_H in the transverse direction [6]. More significantly, Fig. 3 also depicts the variation in $\alpha(\theta)$ and $\xi(\theta)$ for each microstructure condition, both of which seem to strongly contribute to variations in L_H. As can be seen from the evolution of the texture parameter $\alpha(\theta)$ in Fig. 3, random microstructures,

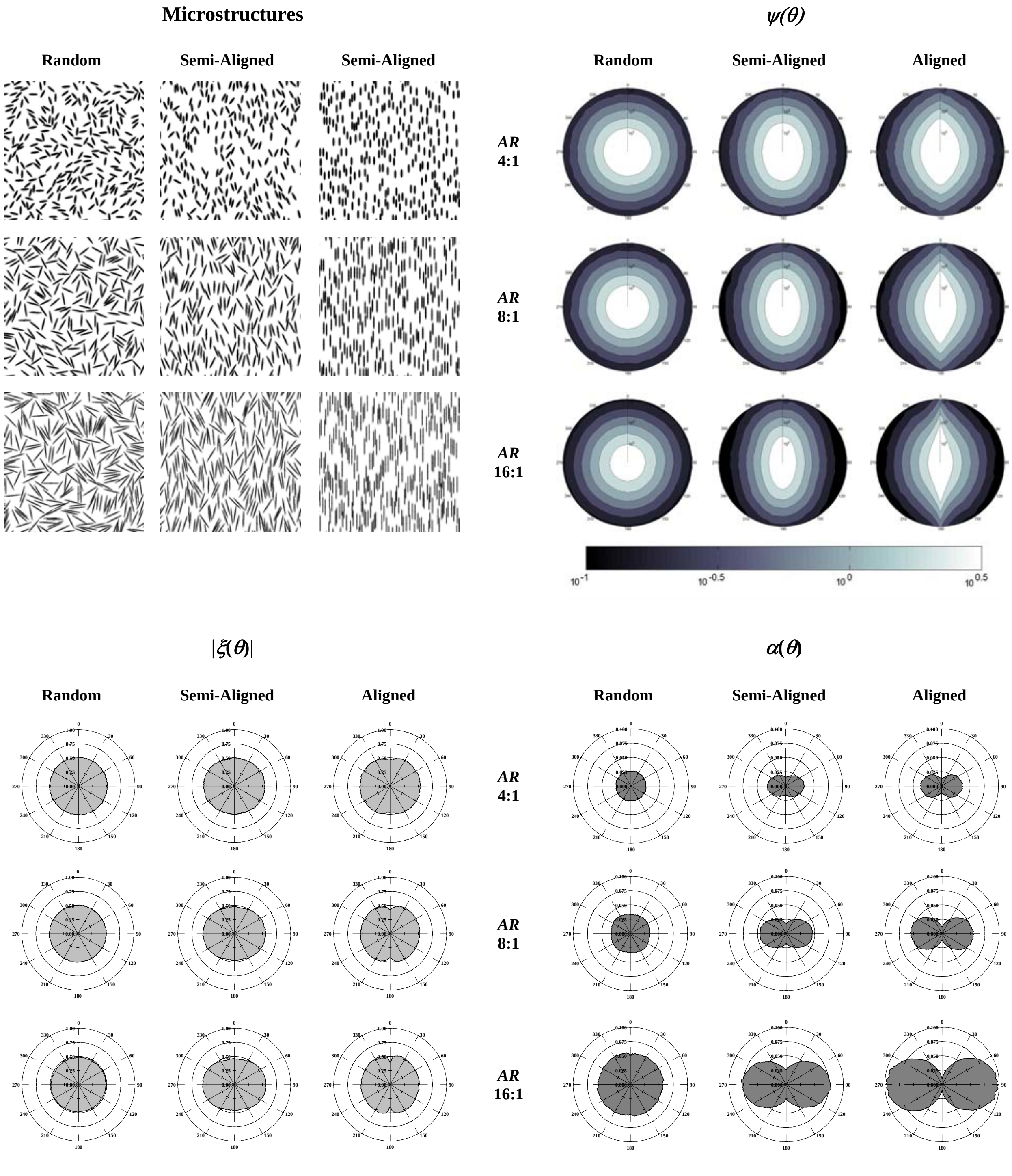

Fig 3. Synthetic microstructures containing $A_f = 20\%$ second-phase and corresponding VMSAAF/$\psi(\theta)$ plots that illustrate the compounded effect of second-phase aspect ratio (*AR*) and major-axis alignment propensity; least squares-fits for the texture and cluster parameters, $\alpha(\theta)$ and $\xi(\theta)$, respectively, are depicted below each microstructure.

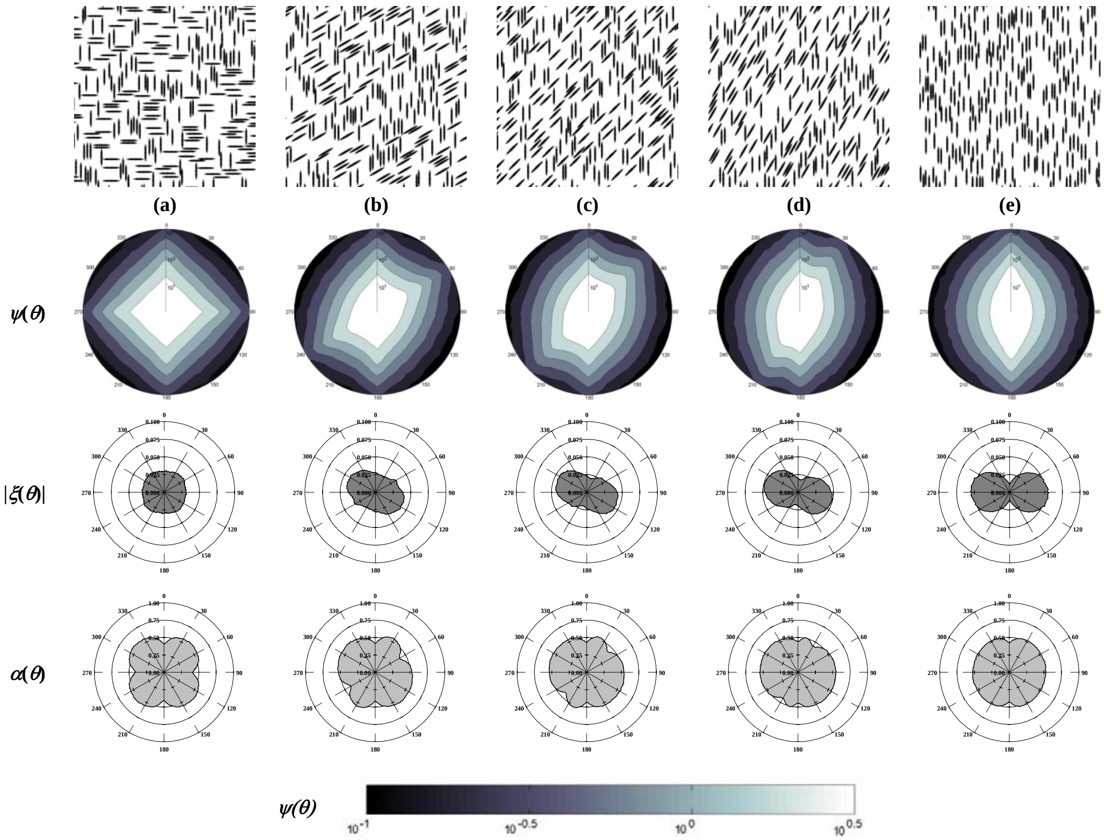

Fig 4. Synthetic microstructures containing A_f = 20 % second phase of aspect ratio 8:1 with specific orientation relationships between 2 equal-fraction variants and corresponding VMSAAF/$\psi(\theta)$ plots for each condition; **(a)** 90° between major particle axes, **(b)** 60°, **(c)** 45°, **(d)** 30°, **(e)** 0°; least squares-fits for the texture and cluster parameters, $\alpha(\theta)$ and $\xi(\theta)$, respectively, are depicted below each microstructure.

regardless of aspect ratio display no directional dependence. However, with increasing alignment propensity of the second phase, deepening cusps appear in α along the direction of alignment ($\theta = 0$). We recognize these as analogs to the rose-plots used to characterize oriented microstructures by Saltykov [13] which, using Underwood's notation [14], are described by

$$\alpha(\theta) = P_L(\theta) = \left(\frac{1}{a}\right)\sin(\theta) + b \tag{3}$$

where $P_L(\theta)$, the probability of intercepting a particle as a function of microstructure angle, can be expressed as the sum of the symmetric (oriented) and isometric (random) components of the microstructure—the ($1/a$) and b terms, respectively—which are reported for all microstructure conditions in Table 1.

The behavior of the cluster parameter, $\xi(\theta)$, as a function of aspect ratio and alignment propensity can also be seen in Fig. 3, and in all conditions depicted is nearly uniform (~ -0.5), except at angles very close to the axis of alignment; a fact qualitatively manifested by the consistent gradients in $\psi(\theta)$ plots at larger length scales, again with the exception of angles near the axis of alignment. Although the general character of these curves is described by an epitrochoid given by

$$\xi(\theta) = \sqrt{(c+d)^2 + h^2 - 2h(c+d)\cos\left(\frac{c}{d}\theta\right)} \tag{4}$$

where the parameters c, d and h—also reported in Table 1—are linked to the shape of this family of curves [15], trends in $\xi(\theta)$ with aspect ratio and alignment propensity are not obvious, and will be the subject of future work.

The behavior of $\xi(\theta)$ at angles near the axis of alignment ($\theta = 0^\circ$) in the aligned microstructures is of particular interest since a representative length-scale measured in the direction of alignment can significantly affect the extent of an RVE constructed from three orthogonal length-scales, and as a consequence, the perception of clustering in a particular microstructure. The deviations from $\xi = 0.5$ in the aligned microstructures suggest that, from a multi-scale perspective—even though particle centroids were placed randomly—there is a propensity for particle clustering in that direction. Evidence of such clustering is observed in the center of the microstructure sub-region depicted in the *aligned* 16:1 microstructure of fig. 3, where a large cluster of particles can be seen in the vertical direction. Tracking this cluster parameter during microstructure generation algorithms like RSA, while cumbersome, may be a way of preventing microstructure clustering without resorting to hard-sphere-type potentials [16]. Deviations from $\xi = 0.5$ in the transverse direction of the *semi-aligned* conditions suggest that the material is less clustered. However, in actuality this is a result of a higher effective area fraction of the second-phase in that direction.

Figure 4 shows the synthetic microstructures with two orientation variants along with their multi-scale behavior. For each condition the variants are distinct and the exact direction of their alignment is clear in the corresponding VMSAAF/$\psi(\theta)$ plots. The presence of more than one variant clearly influences L_H anisotropy in the material, and in particular, the orientation of the minimum representative element required to characterize the microstructure. Although the plots of $\psi(\theta)$ for each condition do not qualitatively resemble what would be expected from the superposition of VMSAAF results for each underlying variant, the plots of $\xi(\theta)$ and $\alpha(\theta)$ resemble the superposition of their constituent variants.

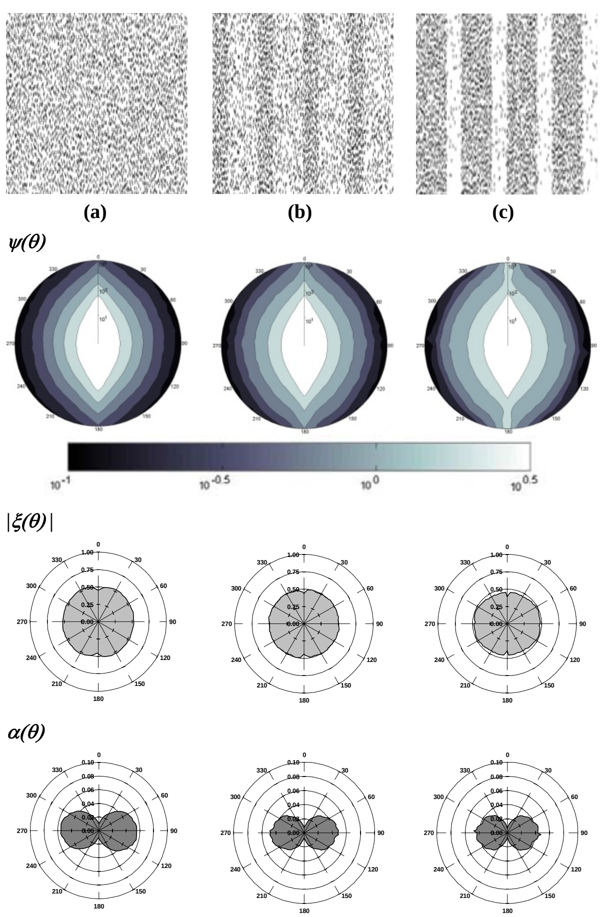

Fig. 5. Effect of microstructure banding on multi-scale behavior in synthetic microstructures containing A_f = 20 % second-phase with an 8:1 aspect ratio with **(a)** no banding, d/r = 0.0 and banding with **(b)** d/r = 0.5 and **(c)** d/r =2.0.

Table 1: Coefficients for describing studied microstructre conditions via the texture $\xi(\theta)$ and cluster $\alpha(\theta)$ parameters using eqs. 3 and 4.

Condition	a	b	c	d	h
Random-AR-4	*	* *		* *	
Random-AR-8	*	* *		* *	
Random-AR-16	*	* *		* *	
Semi-Aligned-AR-4	*	* *		* *	
Semi-Aligned-AR-8	*	* *		* *	
Semi-Aligned-AR-16	*	* *		* *	
Aligned-AR-4	*	* *		* *	
Aligned-AR-8	*	* *		* *	
Aligned-AR-16	*	* *		* *	
Banded-d/r-0.0	*	* *		* *	
Banded-d/r-0.5	*	* *		* *	
Banded-d/r-2.0	*	* *		* *	

That is, if there are n variants in a microstructure and each variant is described by an angle of orientation θ_i, then $\xi(\theta)$ and $\alpha(\theta)$ appear to be given by the relationships

$$\alpha(\theta) = \sum_i^n \left(\frac{1}{a_i}\right)\sin(\theta - \theta_i) + b_i \qquad (5)$$

$$\xi(\theta) = \sum_i^n \sqrt{(c_i + d_i)^2 + h_i^2 - 2h_i(c_i + d_i)\cos\left[\frac{c_i}{d_i}(\theta - \theta_i)\right]} \qquad (6)$$

In conjunction with the previous result that particles cluster very easily along the direction of alignment in aligned microstructures with a single variant, the primary implication of this superposition is that when there are several distinct orientation variants, there will be predetermined directions of clustering for microstructures generated with RSA-like algorithms.

Sample regions of the banded microstructures are depicted in Fig. 5 along with the VMSAAF results for these conditions. From these microstructures, the effect of particle clustering can be distinctly observed even in the presence of second-phase alignment by noticing the shallower gradients in the transverse direction ($\theta = 90^{o}$) of the $\psi(\theta)$ plots as the level of banding is increased (as d/r is increased). The behavior of the texture parameter is similar for all conditions. Interestingly, as the second phase is more strongly segregated into bands, the cluster parameter is reduced regardless of direction (L_H is increasing in every direction), indicating that RVE size would increase significantly because of contributions from all principal axes in the microstructure, not just the components transverse to the band orientation, again suggesting that this may be a very useful parameter for characterizing clustering, especially in oriented materials.

5.) Conclusions

In conclusion, through application to synthetic microstructures with controlled features, it has been shown that the VMSAAF technique presented in this work provides a rapid tool for characterizing key microstructure features, including:

1. Representative length scale (L_H) anisotropy.
2. The presence and orientation of distinct morphological variants through variation in the parameter $\alpha(\theta)$.
3. The presence and orientation of anisotropic clustering through variation in the parameter $\xi(\theta)$.

Acknowledgements

This work is a derivative of GBW's dissertation which was supported by AFOSR (Grant # 01ML05-COR, Program Manager Dr. Joan Fuller).

References

[1] J.Spowart, B.Muryama, D.Miracle, *Mat.Sci.Eng.* A307 (2001),51.
[2] B.Lu, S.Torquato. *J. Chem. Phys.*, 93(1990),3452.
[3] J.Quintanilla, S.Torquato. *J. Chem. Phys.*, 106(1997),2741.
[4] Z.Shan, A.Gohkale. *Comp. Mater. Sci.*, 24(2002),361.
[5] S.Swaminathan, S.Ghosh, N.Pagano, *J. Comp. Mat.*, 40(2006),583.
[6] A.Borbély, P.Kenesei, H.Biermann, *Acta Mater.*, 54(2006), 2735.
[7] J.Spowart, *Mat. Sci. Eng.*,A425(2006),225.
[8] K.Faber, A. Evans, *Acta Metall.*, 31(1983), 565.
[9] K.Faber, A. Evans, *Acta Metall.*, 31(1983), 577.
[10] G.Wilks *Influence of Reinforcement Homogeneity on the Deformation and Fracture of a Discontinuously Reinforced Aluminum Matrix Composite*, PhD Dissertation, Penn State, 2007.
[11] M.Tschopp, G.Wilks, J.Spowart, *Mod. Sim. Mat. Sci.*,16(2008),1.
[12] Where the script can be found
[13] S.Saltykov, *Stereometrc Metallography*, Metallurgizdat, 1958.
[14] E.Underwood, *Quantitative Stereology*, Addison-Wesley, 1970.
[15] J. Lawrence, *A Catalog of Special Plane Curves*. Dover. 1972.
[16] S. Torquato, *Random Heterogeneous Materials Microstructure and Macroscopic Properties*, Springer, 2002.